

Homoclinic tangles, bifurcations and edge stochasticity in diverted tokamaks

T. E. Evans^{*1}, R. K. W. Roeder², J. A. Carter³, and B. I. Rapoport⁴

¹ General Atomics, P.O. Box 85608, San Diego, California, 92186-5608, USA

² Cornell University, Ithaca, New York, USA

³ University of North Carolina, Chapel Hill, North Carolina, USA

⁴ Oxford University, Oxford OX1 3LB, United Kingdom

Received 5 September 2003, accepted 9 February 2004

Published online 23 April 2004

Key words Magnetic stochasticity, homoclinic tangles, pedestal plasma, tokamak.

PACS 05.45.-a, 52.55.Fa, 52.55.Rk, 52.55.-s

The boundary and pedestal region of a poloidally diverted tokamak is particularly susceptible to the onset of vacuum magnetic field stochasticity due to small non-axisymmetric resonant perturbations. Recent calculations of the separatrix topology in diverted tokamaks, when subjected to small magnetic perturbations, show the existence of complex invariant manifold structures known as homoclinic tangles. These structures appear above a relatively low perturbation threshold that depends on certain equilibrium shape parameters. Homoclinic tangles represent a splitting of the unperturbed separatrix into stable and unstable invariant manifolds associated with each X-point (hyperbolic point). The manifolds that make up homoclinic tangles set the boundaries that prescribe how stochastic field line trajectories are organized i.e., how field lines from the inner domain of the unperturbed separatrix mix and are transported to plasma facing surfaces such as divertor target plates and protruding baffle structures. Thus, the topology of these tangles determines which plasma facing components are most likely to interact with escaping magnetic field lines and the parallel heat and particle flux they carry.

© 2004 WILEY-VCH Verlag GmbH & Co. KGaA, Weinheim

1 Introduction

Magnetic field lines in the pedestal region of a poloidally diverted tokamak are particularly susceptible to the onset of global stochasticity due to small resonant perturbations from a variety of non-axisymmetric sources [1]. In a diverted tokamak, poloidal magnetic flux (ψ) escaping the outer edge of this stochastic region is organized by complex topological structures known in nonlinear dynamical systems theory as homoclinic tangles. A tangle can be thought of as a splitting of the separatrix into a set of invariant manifolds when perturbed by small non-axisymmetric magnetic fields. These invariant manifolds form the boundaries that separate field lines with qualitatively different behaviors (e.g. those inside an island versus those outside). An informative discussion of homoclinic tangles found in simple analytic twist maps is given by Guckenheimer and Holmes [2].

Homoclinic tangles are known to play an important role in the global behavior of vector field flows characteristic of conservative Hamiltonian systems. Since the magnetic field in toroidal plasmas may be conveniently represented in terms of a Hamilton-Jacobi (action-angle) formalism, it is natural to analyze such systems with established theories developed for simpler nonlinear systems. In the usual flux coordinate representation of a toroidal system, magnetic field lines can be thought of as guiding center paths for collisionless, drift-free, particles where surfaces of constant ψ correspond to an action in Hamilton's equations. In this representation, the toroidal angle (ϕ) is synonymous with time and the usual poloidal angle (θ) serves as the angular (Hamilton-Jacobi) variable. When using the most straightforward ψ, θ representation, one obtains a set of non-canonical coordinates where the paths of field lines on $\psi(\theta, \phi)$ surfaces are not simple linear functions of θ and ϕ . If required, the system may be transformed into a set of canonical variables but for the purpose of this analysis we use

* Corresponding author: e-mail: evans@fusion.gat.com, Phone: +10 858 455 4269, Fax: +10 858 455 4156

the non-canonical representation since it provides realistic pictures of how tangles interact with plasma facing surfaces in the physical space of interest.

In the following, we present a brief overview of the modeling background (Section 2), followed by a discussion of *resonant* tangles around magnetic islands in the edge plasma region and a discussion of how tangles from one island chain interact with tangles of neighboring island chains (Section 3). These resonant island-to-island tangle intersections provide non-diffusive transport paths that mix the magnetic flux across the outer stochastic region of the plasma. We conclude Section 3 with calculations of *non-resonant* homoclinic tangles that make up the primary separatrix of a perturbed poloidally diverted equilibrium and discuss how field lines lost from the stochastic region are guided to plasma facing surfaces by these primary separatrix tangles. Since homoclinic tangles play an important role in the transport of particles and energy out of the pedestal plasma, when small magnetic perturbations are present in the system, our goal is predict the properties of tangles with changes in the perturbation and equilibrium characteristics. We summarize the conclusions in Section 4.

2 Modeling background

Mapping codes are commonly used in nonlinear dynamical systems theory to study the global behavior of a system's phase space. They are used to iterate sets of solutions to differential equations through a fixed time step. In other words, they map solutions from one surface-of-section to subsequent solutions under forward, one-to-one, iterations of the map and backward to previous solution surfaces under inverse iterations. These mapping codes provide powerful tools for understanding the dynamics of nonlinear systems and are used extensively to study "analytic" twist maps such as those discussed in Ref. [2]. Since "analytic" mapping codes are impractical for modeling field lines in realistic poloidally diverted tokamaks with non-circular flux surfaces and safety factor profiles determined by plasma profiles, we have chosen to use numerical mapping codes for these studies. This has two distinct advantages over analytic mapping codes. No assumptions are required on the toroidal symmetry of the perturbation source and realistic pressure/current profiles consistent with Grad-Shafranov equilibrium solvers, are easily incorporated into the modeling.

The modeling discussed in this paper is based on a set of 3D magnetic field line integration codes, known as TRIPND and TRIP3D, that are used to study stochastic boundary layers in limiter and diverted tokamaks respectively. These codes, previously discussed in greater detail in Ref. [1], have been converted into a set of mapping codes using a MatLab [3] interface and coupled to an algorithm that computes the invariant manifolds for each X-(hyperbolic) point of the system. The mapping code associated with TRIPND is referred to as TRIP_MAP and that associated with TRIP3D is referred to as TRIP3D_MAP in this paper.

It should be recalled that (un)stable invariant manifolds of a nonlinear system are divided into two sets representing the generalized eigenspaces associated with a hyperbolic fixed point or X-point. The eigenvalues associated with a hyperbolic fixed point χ_h are λ_s , the stable eigenvalue, satisfying $|\lambda_s| < 1$ and λ_u , the unstable eigenvalue, satisfying $|\lambda_u| > 1$. These eigenvalues define the eigenvectors of the stable manifold $W^s(\chi_h)$ and the unstable manifold $W^u(\chi_h)$ respectively. We informally define the (un)stable manifold for a given hyperbolic fixed point χ_h of a map f as follows:

$$W^u(\chi_h) = \{\chi | \lim_{n \rightarrow \infty} f^{-n}(\chi) = \chi_h\}, \quad (1)$$

and

$$W^s(\chi_h) = \{\chi | \lim_{n \rightarrow \infty} f^n(\chi) = \chi_h\}. \quad (2)$$

Here, we see that solution trajectories approach χ_h along the stable manifold $W^s(\chi_h)$ and veer away from χ_h as they leave along the unstable manifold $W^u(\chi_h)$. In terms of our time-like variable ϕ , the solution trajectories asymptotically approach $W^u(\chi_h)$ for forward mappings while for inverse mappings the solution trajectories asymptotically approach the $W^s(\chi_h)$. Thus the stable manifold of χ_h is defined as the set of initial conditions χ_0 such that $\chi(\phi) \rightarrow \chi_h$ as $\phi \rightarrow \infty$ while the unstable manifold is the set of initial conditions such that $\chi(\phi) \rightarrow \chi_h$ as $\phi \rightarrow -\infty$. Note that a typical trajectory asymptotically approach the unstable manifold as $\phi \rightarrow \infty$, and the stable manifold as $\phi \rightarrow -\infty$. Since each X-point has a pair of stable and unstable invariant manifolds associated with it, the mapping algorithm first determines the four eigenvectors and uses the directions of these to map line segments backward along the stable manifolds and forward along the unstable manifolds. This results in two sets of stable and unstable manifolds (one on each side of the X-point).

It is important to realize that poloidally diverted systems have two types of X-points, resonant X-points associated with individual helical harmonics of the perturbation sources, and non-resonant x-points that result from a linear superposition of all the non-axisymmetric perturbations present in the system. Resonant X-points are associated with helical magnetic islands on rational surfaces while non-resonant X-points are associated with axisymmetric fixed points that define the stable and unstable manifolds making up the primary separatrix. Unperturbed or integrable systems have axisymmetric flux surfaces bounded by sets of stable and unstable invariant manifolds that intersect identically at every point forming the usual axisymmetric separatrix picture. When small non-axisymmetric perturbations are present in the system, the stable and unstable manifolds split and intersect transversely at homoclinic points forming a homoclinic tangle. Once the separatrix splits there are infinitely many homoclinic points that accumulate as the X-point is approached along the stable and unstable manifold from each side. The web formed by the stable and unstable invariant manifolds undergoing these intersections is known as a homoclinic tangle. It is the intersection of these wildly oscillating stable and unstable manifolds with each other near the X-points that is responsible for the onset of stochasticity in the vicinity of the X-points at relatively low perturbation levels.

3 Results and Discussion

A fundamental source of non-axisymmetric perturbations, present in all tokamaks, is produced by small random mechanical variations in the positions and shapes of all the magnetic field coils, current feeds, and magnetic materials comprising the system (i.e., ensemble effects). These are inherent in any magnetic confinement system due to the build up of engineering tolerances, thermal stresses, and small mechanical vibrations. Individually they are small enough that they typically fall below the resolution of measuring instruments used to quantify “error fields” due to macroscopic shifts and tilts of individual coils. We note that in DIII-D “error fields”, due to the poloidal field coils, have been measured [4] but relatively little is known about ensemble effects since these are difficult to model in poloidally diverted equilibria. Collectively, ensemble effects can produce substantial amounts of edge stochasticity in limiter tokamaks. Using statistical methods it has been shown that ensemble or Intrinsic Topological Noise (ITN) sources drive the formation of resonant islands comparable to those produced by “error fields” [5].

In Fig. 1, we show a broad stochastic region with remnant $q = 1, 2$ and 3 island chains in a limiter plasma configuration perturbed by random radial displacements of the toroidal field coils. Here, the Gaussian random normal standard deviation, about the axisymmetric mean, is approximately the same size as a typical poloidal field coil shift in DIII-D. As pointed out in Ref. [5], small random shifts of toroidal field coils produce significantly larger resonant effects than comparable shifts in the other coils that make up the system. For this case, field lines calculated with the TRIP_MAP code are represented by the dots in Fig. 1(a) and are strongly stochastic between the remnant island chains. Homoclinic tangles for individual islands in the $m, n = 1, 1; 2, 1; \text{ and } 3, 1$ chains are also superimposed on several island remnants (solid lines) in Fig. 1(a). The homoclinic tangles shown in Fig. 1 are formed by the intersection of the stable and unstable manifolds and calculated with the TRIP_MAP algorithm discussed in Sec. 2. Enlargements of these resonant island tangles are shown in Figs. 1(b), 1(c) and 1(d), respectively. Note the intersections of stable and unstable manifolds within each island chain. These produce stochastic orbits near the X-points and in the vicinity of the resonant separatrices. The large island chain tangles also intersect smaller island chain tangles in the regions between the primary resonances (not shown in the figure) creating stochasticity and mixing from one chain to another. This island-to-island overlap of stable (unstable) manifolds from one chain with unstable (stable) manifolds of a neighboring chain is the mechanism responsible for the onset of global stochasticity. Thus, the approximate form of the Chirikov overlap condition [6], commonly quoted in the literature, must be modified to account for the effects of these homoclinic tangle intersections. This is quite clear because stable (unstable) manifolds from one island chain may not intersect stable (unstable) manifolds from a neighboring island chain as is implied by the simplified Chirikov picture.

Resonant island tangles, similar to those shown in Fig. 1 have also been calculated in DIII-D equilibria perturbed by a set of non-axisymmetric “error correction” coils [7]. These calculations are done in TRIP3D_MAP using an axisymmetric Grad-Shafranov equilibrium and perturbation fields calculated with a Biot-Savart algorithm. In DIII-D controlled non-axisymmetric perturbations are produced by a set of external “error field” correction coils (C-coils) [8] and a set of internal resistive wall feedback coils (I-coils) [9]. Non-axisymmetric “error fields”

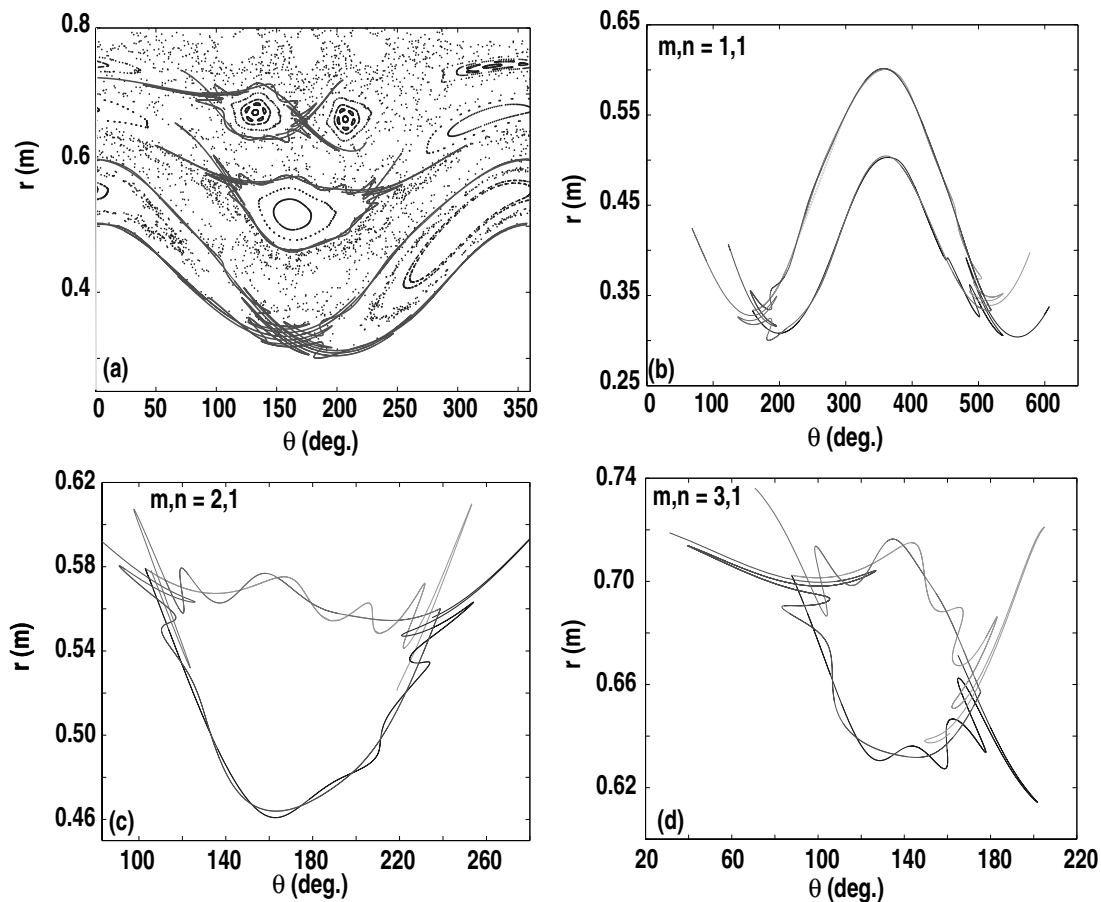


Fig. 1 (a) Phase portrait of a circular plasma equilibrium with black dots representing field lines and solid curves representing the invariant manifolds making up homoclinic tangles. A full view of $m, n = 1, 1$ island tangles (b) without field lines plotted over two poloidal periods to show the tangles on each side of the X-point and expanded views of $m, n = 2, 1$ island tangles (c) and $m, n = 3, 1$ homoclinic tangles (d) without field lines from the TRIP_MAP code at a relatively high perturbation level.

due to shifted poloidal field coils are also included in TRIP3D_MAP. The edge stochastic region produced by “error fields” from poloidal field coil shifts is expected to be relatively small compared to that from the C-coil which is designed to null “error fields” on the $q = 2$ surface. Nevertheless, both these and ITN sources which have yet to be fully modeled contribute to the global stochasticity in DIII-D. Here again, it is the island-to-island homoclinic tangle intersections that determine how field lines mix and are transported out to the plasma edge.

At the outer edge of the pedestal region, in poloidally diverted tokamaks, stochastic field line escape pathways are opened when stable (unstable) manifolds due to resonant island tangles intersect unstable (stable) manifold formed by non-resonant primary separatrix tangles. Thus, it is the non-resonant tangles that determine where the escaping flux interacts with plasma facing surfaces. The topology of these non-resonant tangles is sensitive to various equilibrium shape parameters such as: triangularity, squareness, up-down X-point balance (i.e., dR_{sep}) and position, as well as the properties of the perturbation source. For example, with a given dR_{sep} (a relative measure of the up-down symmetry) as the current in the C-coils is increased we first see small tangles appear at the dominate X-point. These tangles are first visible at C-coil currents which are about an order of magnitude smaller than those typically required to cancel error fields from the poloidal field coils on the $q = 2$ surface and are formed by both the stable and unstable manifolds of the dominate X-point. The stable manifold from the secondary X-point, displaced by the flux expansion near the dominate X-point, also has a small spatial oscillation at this perturbation level while the corresponding unstable manifold is relatively unaffected. This is the first step in a complex homoclinic bifurcation sequence observed as the C-coil current is increased. An example of

this effect is shown in Fig. 2 of Ref. [7]. Eventually complex tangles can develop either at both X-points or predominately at one X-point depending on the values of various equilibrium shape parameters.

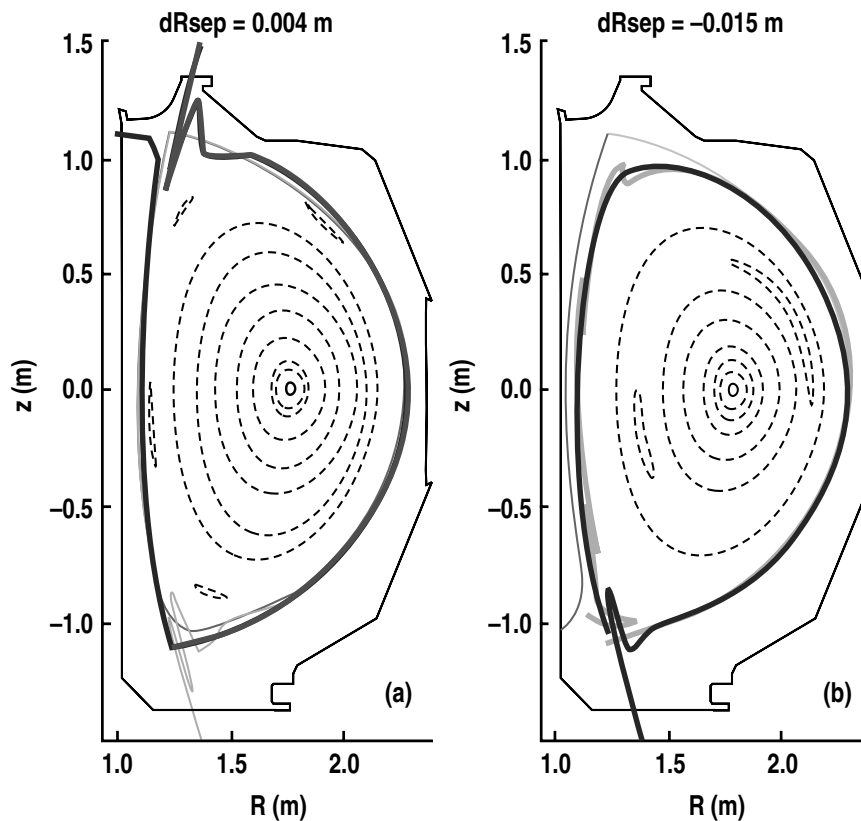


Fig. 2 Bifurcations in non-resonant separatrix tangles with a constant C-coil current of 10,000 amp-turns for (a) $dR_{sep} = 0.004$ m and (b) $dR_{sep} = -0.015$ m.

The sensitivity of these tangle bifurcation sequences to the dR_{sep} parameter is shown in Fig. 2. Here the C-coil current is fixed at 10,000 amp-turns and dR_{sep} is varied by less than 0.02 m from slightly upward biased [Fig. 2(a) with $dR_{sep} = 0.004$ m] to downward biased [Fig. 2(b) with $dR_{sep} = -0.015$ m]. The invariant manifolds from each X-point display a complex sequence of bifurcations that direct escaping magnetic flux from the pedestal region onto significantly different plasma facing surfaces. In Fig. 2(a), with a relatively small positive dR_{sep} parameter, the tips of several large tangles approach the divertor target plates at radial locations outside the usual strike point position. The size of these tangles generally change with toroidal angle producing a spiral-like footprint on the target plates [7]. Moving along the divertor target plate surfaces toward smaller major radius (R) from the outer edge, we encounter an infinite number of narrower, more closely spaced, tangles that make up the primary outer strike points. Due to the resolution of the calculations we have not shown the fine structure that exists near the strike points. This fine structure suggests that very narrow regions near the strike points can be connected to field lines that penetrate deep into the pedestal region and carry significantly more energy than expected from the usual scrape-off layer picture.

The patterns displayed by non-resonant homoclinic tangles, such as those seen in Fig. 2, are strongly suggestive of experimentally measured, toroidally asymmetric, divertor heat flux profiles seen in DIII-D [10]. The heat flux data sometimes shows multiple peaks at one toroidal angle while a single peak is seen simultaneously at another toroidal angle. These bifurcated heat flux peaks are typically more common in plasmas with a small dR_{sep} parameter as suggested by the homoclinic tangle topology shown in Fig. 2(a). It should be noted that the calculations presented in Fig. 2 only include perturbations from the C-coil with a common level of current that is routinely used in DIII-D. When perturbations from “error fields” due to shifted poloidal field coils are included

in the calculation, the topology of the tangles is much more complex and the size of the individual tangle lobes increase as perturbation sources are added to the calculations. This implies that magnetic system ensemble or ITN sources discussed above can also be expected make a significant contribution to the overall topology of the tangles.

4 Conclusions

Two types of homoclinic tangles have been identified in magnetically perturbed, diverted tokamaks. Resonant magnetic island tangles produce both local (X -point and island separatrix) stochasticity and are responsible for the onset of global stochasticity in the pedestal region of the plasma. Non-resonant separatrix tangles, associated with axisymmetric X -points, determine which plasma facing surfaces intercept the magnetic flux lost from the resonant stochastic region. All toroidal confinement systems are subject to the effects of resonant homoclinic tangle stochasticity and magnetic flux loss across the boundary region to plasma facing surfaces but poloidally diverted tokamaks also have non-resonant homoclinic tangles with complex bifurcation sequences of their own. The net effect is that poloidally diverted tokamaks are much more susceptible to edge stochastic magnetic flux loss but the escaping flux is relatively well focused onto small surface regions in the vicinity of the divertors.

Since small magnetic perturbations, such as system ensemble or intrinsic topological noise sources discussed above, are unavoidable in toroidal magnetic confinement systems, the physics of the edge plasma is inherently 3D. This fact needs to be considered when interpreting experimental measurements and modeling edge plasmas. This is particularly true in poloidally diverted plasmas where such effects are much more pronounced.

Acknowledgements The work discussed in this paper was sponsored by the U.S. Department of Energy under Contract Nos. DE-AC03-99ER54463 and W-7405-ENG-48. Support for R.K.W.R. was also provided by a NDSEG Fellowship and for J.A.C. and B.I.R. through the DoE National Undergraduate Fusion Fellowship Program.

References

- [1] T.E. Evans, R.A. Moyer, P. Monat, *Phys. Plasmas* **9**, 4957 (2002).
- [2] J. Guckenheimer, P. Holmes, *Nonlinear Oscillations, Dynamical Systems, and Bifurcations of Vector Fields*, Applied Mathematical Science **42** (Springer-Verlag, New York, 1983) p. 45.
- [3] The MathWorks, Inc., 3 Apple Hill Dr., Natic, Massachusetts 01760.
- [4] J.L. Luxon, M.J. Schaffer, G.L. Jackson, et al., "Anomalies in the Applied Magnetic Fields on DIII-D and their Implications for the Understanding of Stability Experiments," submitted to *Nucl. Fusion* (2003).
- [5] T.E. Evans, Proceedings of the 18th European Physical Society Conference on Controlled Fusion and Plasma Physics, Berlin, Germany, 1991 (European Physical Society, Petit-Lancy, 1991), Part II, p. 65
- [6] B.V. Chirikov, *Phys. Rep.* **52**, 263 (1979).
- [7] R.K.W. Roeder, B.I. Rapoport, T.E. Evans, *Phys. Plasmas* **10**, 3796 (2003).
- [8] J.T. Scoville, R.J. La Haye, Proceedings of the 14th IEEE/NPSS Symposium on Fusion Engineering, San Diego, California, 1991 (Institute of Electrical and Electronics Engineers, Inc., Piscataway, New Jersey, 1992), Vol. II, p. 1144.
- [9] G.L. Jackson, P.M. Anderson, J. Bialek, et al., Proceedings of the 30th European Physical Society Conference on Controlled Fusion and Plasma Physics, St Petersburg, Russia, 2003, paper P-4.47 on CD-ROM.
- [10] T.E. Evans, C.J. Lasnier, D.N. Hill, et al., *J. Nucl. Mater.* **220-222**, 235 (1995).